Coatomer protein complex subunit ζ1 expression is associated with postoperative outcomes and endoplasmic reticulum stress-related changes in hepatocellular carcinoma

TAKUYA KATO[1], TATSUYA ORIMO[1], YOH ASAHI[1], YUKI FUJII[1], KANAKO C. HATANAKA[2], AKIHISA NAGATSU[1], TAKESHI AIYAMA[1], TATSUHIKO KAKISAKA[1], YUTAKA HATANAKA[2] and AKINOBU TAKETOMI[1]

[1]Department of Gastroenterological Surgery I, Hokkaido University Graduate School of Medicine, Sapporo, Hokkaido 060-8648, Japan; [2]Center for Development of Advanced Diagnostics, Hokkaido University Hospital, Sapporo, Hokkaido 060-8638, Japan

Received May 27, 2026; Accepted October 6, 2026

DOI: 10.3892/ol.2026.15950

Abstract. Hepatocellular carcinoma (HCC) has a high recurrence rate and limited therapeutic targets. Although coatomer protein complex subunit ζ1 (COPZ1) has been identified as a potential therapeutic target based on non-oncogene addiction in other types of cancer, its role in HCC progression remains unclear; therefore, COPZ1 expression was evaluated in the present study by immunohistochemistry in 227 resected HCC specimens, and its associations with clinicopathological features and survival were analyzed. In addition, the functional effects of COPZ1 knockdown were assessed in PLC/PRF/5 and HLF HCC cell lines. COPZ1 was highly expressed in 60.3% of tumors, and was independently associated with shorter disease-free survival (DFS) and overall survival (OS). The COPZ1-high and COPZ1-low groups had median DFS times of 12.0 and 24.1 months, and 5-year OS rates of 63.7 and 80.1%, respectively. COPZ1 knockdown significantly reduced cell proliferation (P<0.001), migration (P<0.001) and invasion (P<0.01). Furthermore, RNA sequencing identified >1,600 differentially expressed genes enriched in unfolded protein response pathways; this was confirmed by a gene set enrichment analysis. In addition, under endoplasmic reticulum stress, COPZ1 knockdown was associated with changes in ER stress-related proteins. In conclusion, COPZ1 expression is associated with poor postoperative outcomes in HCC and its knockdown can suppress malignant phenotypes in HCC cells, supporting its biological relevance and warranting further investigation of its therapeutic relevance.

Correspondence to: Dr Yoh Asahi, Department of Gastroenterological Surgery I, Hokkaido University Graduate School of Medicine, Kita 14, Nishi 5, Kita, Sapporo, Hokkaido 060-8648, Japan
E-mail: yasahi@pop.med.hokudai.ac.jp

Abbreviations: AFP, α-fetoprotein; BCV, biological coefficient of variation; CI, confidence interval; COPI, coat protein complex I; COPZ1, coatomer protein complex subunit ζ1; DEG, differentially expressed gene; DFS, disease-free survival; eIF2α, eukaryotic translation initiation factor 2α; ER, endoplasmic reticulum; FDR, false discovery rate; GADD34, growth arrest and DNA damage-inducible protein 34; GSEA, gene set enrichment analysis; HCC, hepatocellular carcinoma; HR, hazard ratio; IHC, immunohistochemistry; IRE1, inositol-requiring enzyme 1; KD, knockdown; NES, normalized enrichment score; OS, overall survival; PCA, principal component analysis; p-, phosphorylated; PERK, protein kinase RNA-like endoplasmic reticulum kinase; RNA-seq, RNA sequencing; siRNA, small interfering RNA; UPR, unfolded protein response

Key words: HCC, COPZ1, liver resection, UPR, RNA-seq

Introduction

Hepatocellular carcinoma (HCC) accounts for 75-80% of primary liver cancer cases (1), and it ranks as the sixth most commonly diagnosed cancer and third-highest cause of cancer-related deaths worldwide (2). Despite the high global burden of HCC and recent advances in systemic treatment methods, effective therapeutic strategies remain limited.

One reason for the poor prognosis of patients with HCC is the limited efficacy of the currently available systemic therapies. These therapies include tyrosine kinase inhibitors and immune checkpoint inhibitors, which are the current standard treatments for advanced HCC. HCC is often asymptomatic in its early stages. Therefore, HCC is frequently diagnosed at an advanced stage (3), where systemic therapy becomes the main treatment option (4). Furthermore, HCC has a high recurrence rate following liver resection, and systemic therapy may be required for patients who develop unresectable recurrence (5-7). Despite the substantial progress in systemic therapies for HCC and the large number of patients eligible for such treatments, disease progression during therapy remains common (8-12). Therefore, identifying novel targets for systemic therapy is essential to further improve advanced survival outcomes of patients with HCC.

Coat protein complex I (COPI), which is primarily involved in membrane trafficking between the endoplasmic

reticulum (ER) and Golgi apparatus, has been implicated in autophagy (13), maintenance of lipid homeostasis (14), and iron metabolism (15) within the cell. Coatomer protein complex subunit ζ1 (COPZ1) is one subunit of COPI with a molecular weight of approximately 20 kDa and was identified in the 1990s (16). COPZ1 has been identified as a potential non-oncogene addiction target, with studies in thyroid cancer and lung adenocarcinoma demonstrating that its inhibition can suppress tumor progression (17,18). According to a previous comprehensive proteomic analysis, COPZ1 expression levels were upregulated in poorly differentiated HCC (19), together with other molecules, such as end-binding protein 1, vimentin, S100 calcium-binding protein A9, and proliferating cell nuclear antigen. These molecules are associated with aggressive clinical features in patients with HCC (20-23). These findings suggest that COPZ1 is involved in aggressive tumor behavior in HCC and it warrants further investigation as a candidate for therapeutic vulnerability. However, how COPZ1 is involved in HCC progression remains unclear.

Therefore, we focused on COPZ1 as a candidate molecule of interest for identifying novel therapeutic vulnerabilities in HCC. In the present study, we aimed to determine the clinical and biological relevance of COPZ1 in HCC by examining its association with postoperative outcomes and evaluating the effects of COPZ1 knockdown (COPZ1-KD) in HCC cell lines.

Materials and methods

Patients. This study involved patients with HCC who underwent potentially curative liver resection from January 2008 to December 2014 in the Department of Gastroenterological Surgery I, Hokkaido University Hospital (Sapporo, Japan). The exclusion criteria were as follows: i) Preoperative treatment history; ii) presence of malignant diseases other than HCC; and iii) death from other causes. The Hokkaido University algorithm for hepatic resection was followed for patients (24). Follow-up of patients after liver resection was performed with imaging studies and measurements of α-fetoprotein (AFP) concentrations and protein induced by des-γ-carboxy prothrombin every 3-6 months. The study included 184 male and 43 female patients, with a median age of 66 years (range, 34-86 years).

This study was approved by the institutional board of Hokkaido University Hospital (approval no. 019-0060; Sapporo, Japan) and conducted in accordance with the Declaration of Helsinki. Informed consent was obtained using an opt-out approach.

Immunohistochemistry (IHC). IHC assays were performed on resected HCC tissues. Tissue sections (4 μm thick) were deparaffinized in xylene and rehydrated through a graded ethanol series. Antigen retrieval was carried out in a high pH antigen retrieval buffer (Dako, Glostrup, Denmark) using the PT LINK system (Dako) for 20 min at 97˚C. Endogenous peroxidase activity was blocked with peroxidase-blocking reagent (Dako) for 5 min at room temperature. The sections were then incubated with a rabbit polyclonal anti-COPZ1 antibody (1:400, SAB4500896; Sigma-Aldrich, St Louis, MO, USA) for 30 min at 25˚C. After further incubation with EnVision FLEX/HRP (Dako), the sections were visualized using EnVision FLEX DAB+ (Dako). Lung cancer cells (LK-2) were used as positive controls and lymphoblast-like cells (SU-DHL-6) as negative controls (Fig. S1).

IHC examinations were performed by two observers (TK and KCH, experienced pathologists) who were blinded to the clinical features of the patients with HCC. Discrepant scores between the two observers were reviewed jointly, and a final score was determined by consensus. Formal assessment of interobserver agreement was not performed. The COPZ1 IHC staining intensity in tumor areas was classified as very weak (score, 0), weak (score, 1), moderate (score, 2), or strong (score, 3). Cases with staining scores of 0 or 1 were defined as the COPZ1-low group, while those with scores of 2 or 3 were defined as the COPZ1-high group. The cutoff was selected to distinguish absent-to-weak staining (scores 0-1) from moderate-to-strong staining (scores 2-3).

Cell culture. Human HCC cell lines (PLC/PRF/5 and HLF) were cultured in Dulbecco's Modified Eagle Medium (Nacalai, Kyoto, Japan) supplemented with 10% fetal bovine serum (Sigma-Aldrich) and 1% penicillin/streptomycin (Nacalai) in an incubator containing 5% CO_2 at 37˚C. PLC/PRF/5 cells (JCRB0406; CVCL_0485) were obtained from the JCRB Cell Bank (https://cellbank.nibn.go.jp/~cellbank/en/search_res_det.cgi?ID=388) in 2013. HLF cells were established at Kurume University in 1984 and were kindly provided by the National Cancer Center Research Institute (Tokyo, Japan) in 2015. All cell lines were stocked in the vapor phase above liquid nitrogen immediately after acquisition and passaged for no longer than 6 months. Authentication of these cell lines was performed using short-tandem repeat profiling by the providers. The number of cells was counted using a Countess II Automated Cell Counter (Invitrogen, Carlsbad, CA, USA).

Small interfering (si)RNA treatment. A non-targeting siRNA (siNC; cat. no. 4390843) and a COPZ1-targeting siRNA (siCOPZ1; assay ID s22429, cat. no. 4392420) were obtained from Thermo Fisher Scientific (Waltham, MA, USA). The nucleotide sequence of siNC is proprietary and is not disclosed by the manufacturer. The sequences of siCOPZ1 were 5'-CCA UCGGACUGACAGUGAAtt-3' (sense) and 5'-UUCACUGUC AGUCCGAUGGgt-3' (antisense). The cells were transfected with 20 nM of each siRNA using Lipofectamine RNAiMAX (Thermo Fisher Scientific) for 48 h. Cells transfected with siNC served as controls in all siRNA experiments.

Western blot analysis. HCC cells ($5x10^3$ cells/well) were cultured in a six-well plate and treated with the non-targeting siRNA or COPZ1-targeting siRNA for 48 h before cell protein extraction. Proteins were extracted from cultured cells by homogenization in a lysis buffer (25 mM Tris-HCl, pH 7.5; 150 mM NaCl; 0.5% sodium deoxycholate; 1 mM EDTA; 0.5% NP-40; 5 mM NaF; 5 mM sodium orthovanadate) supplemented with a protease inhibitor cocktail (Sigma-Aldrich). The proteins were subjected to sodium dodecyl sulfate-polyacrylamide gel electrophoresis and immunoblotting. The membranes were blocked with 3% skim milk and incubated for 16 h at 4˚C with the following primary antibodies: Rabbit polyclonal anti-COPZ1 (SAB4500896, 1:1,000; Sigma-Aldrich), rabbit anti-protein kinase RNA-like endoplasmic reticulum kinase

(PERK) (#3192, 1:1,000; Cell Signaling Technology), rabbit anti-p-PERK (#3179, 1:1,000; Cell Signaling Technology), rabbit anti- eukaryotic translation initiation factor 2α (eIF2α; #5324, 1:1,000; Cell Signaling Technology), rabbit anti-p-eIF2α (#3597, 1:1,000; Cell Signaling Technology), rabbit anti-growth arrest and DNA damage-inducible protein 34 (GADD34) (#41222, 1:1,000; Cell Signaling Technology), rabbit anti-inositol-requiring enzyme 1 (IRE1; #3294, 1:1,000; Cell Signaling Technology), rabbit anti-α-tubulin (#2125, 1:1,000, Cell Signaling Technology), and rabbit anti-b-actin (#8457, 1:1,000, Cell Signaling Technology). β-actin and α-tubulin were used as loading controls. The membranes were then incubated for 1 h at 25˚C with a horseradish peroxidase-conjugated secondary antibody (#7074, 1:5,000; Cell Signaling Technology). Protein bands were visualized with the SuperSignal West Dura Extended Duration Substrate (Thermo Fisher Scientific) using the ChemiDoc XRS Plus System with Image Lab (BIO-RAD, Hercules, CA, USA).

Proliferation assay. Proliferation assays were performed using the Cell Counting Kit-8 (Dojindo Laboratories, Kumamoto, Japan) according to the manufacturer's instructions. HCC cells in a 96-well plate ($5x10^3$ cells/well) were treated with the non-targeting siRNA or COPZ1-targeting siRNA for 24-96 h. Cell Counting Kit-8 solution (10 μl) was then added to each well, and the cells were further incubated for 2 h at 37˚C. The absorbance values were measured at 450 nm using Varioskan Flash (Thermo Fisher Scientific).

Wound healing assay. Cell monolayers ($5x10^4$ cells/well) were grown to 90% confluence in a 24-well plate and scratched with a 200-μl pipette tip. After washing with phosphate-buffered saline, the cells were incubated in serum-free medium with the non-targeting siRNA or COPZ1-targeting siRNA for 24 h. The area of the scratched region was measured using ImageJ software (National Institutes of Health, Bethesda, MD, USA).

Invasion assay. Invasion assays were performed on 24-well Matrigel invasion chambers with 8-μm pores (Corning, Corning, NY, USA). Cells ($5x10^4$) were seeded into the upper chambers and incubated with the non-targeting siRNA or COPZ1-targeting siRNA for 24 h. The non-invading cells were then removed using a cotton-tipped swab, and the membranes were fixed and stained using a Diff-Quik kit (Sysmex, Kobe, Japan). The invaded cells were counted under a microscope in five randomly selected fields at x200 magnification. All functional assays were performed independently three times (n=3 biological replicates).

RNA extraction, genome-wide transcriptomic profiling, and gene set enrichment analysis (GSEA). A comprehensive transcriptomic analysis was performed using RNA sequencing (RNA-seq) to compare the gene expression profiles between control siRNA-treated HCC cells and COPZ1-KD HCC cells. HCC cells ($5x10^3$ cells/well) were cultured in a six-well plate and treated with the non-targeting siRNA or COPZ1-targeting siRNA for 48 h. Total RNA was extracted from each cell line using the RNeasy Plus Mini kit (Qiagen, Hilden, Germany). RNA-seq was performed using two independent biological replicates for each condition. The library preparation, RNA-seq, and subsequent data analysis were performed by Rhelixa, Inc. (Tokyo, Japan). Strand-specific, poly-A-selected libraries were sequenced on the Illumina NovaSeq 6000 platform (Illumina, San Diego, CA, USA), generating approximately 26.7 million paired-end reads (2x150 base pairs) per sample. The RNA-seq data generated in the present study have been submitted to the DDBJ Sequence Read Archive under BioProject accession number PRJDB42197. Differentially expressed genes (DEGs) were identified using a Benjamini-Hochberg adjusted P-value threshold of <0.01, without applying fold-change cutoffs. Reproducibility between replicates was assessed separately within each cell line on variance-stabilizing-transformed counts, by principal component analysis (PCA) of the 500 most variable genes, pairwise Pearson correlation across expressed genes (mean normalized count ≥10), and the biological coefficient of variation (BCV), calculated as the square root of the gene-wise dispersion estimate. An enrichment analysis of the DEGs commonly detected in PLC/PRF/5 and HLF cells was performed using the Enrichr platform (https://maayanlab.cloud/Enrichr/), with referencing of the MSigDB Hallmark 2020 gene set database. An adjusted P<0.05 was considered statistically significant in the enrichment analysis. A GSEA was performed using GSEA v4.2.3 (Broad Institute) with 1,000 permutations under the classic scoring scheme, using the h.all.v2024.1.Hs.symbols.gmt gene set.

Stress marker analysis and apoptosis assay. To investigate the role of COPZ1 in response to ER stress, a stress marker analysis was performed. HCC cells ($5x10^3$ cells/well) were cultured in a six-well plate and treated with the non-targeting siRNA or COPZ1-targeting siRNA for 48 h, followed by 24 h of ER stress induced by thapsigargin (#12758, 1 μM; Cell Signaling) treatment. A western blot analysis was performed using antibodies against COPZ1, PERK, phosphorylated PERK (p-PERK), eIF2α, phosphorylated eIF2α (p-eIF2α), GADD34, and α-tubulin.

Apoptosis levels were assessed using the Caspase-3/7 Green Detection Reagent (CellEvent, Invitrogen), according to the manufacturer's protocol, following 24 h of ER stress.

Statistical analysis. All data are presented as the mean ± standard deviation. Statistical analyses were performed using the two-sided unpaired Student's t-test for continuous variables and Pearson's χ^2 test for categorical variables. For densitometric analyses of western blots, protein expression levels were normalized to α-tubulin and expressed relative to the control in each experiment; because this normalization results in unequal variances between groups, comparisons between control siRNA-treated and COPZ1-KD cells were performed using the two-sided Welch's t-test. Disease-free survival (DFS) was defined as the time from liver resection to the first documented recurrence or death, with patients without recurrence censored at the last follow-up. Overall survival (OS) was defined as the time from liver resection to death from any cause, with surviving patients censored at the last follow-up. Survival curves were evaluated using the Kaplan-Meier method and compared using the log-rank test. Univariate and multivariate survival analyses were performed using the Cox proportional hazards model. The proportional hazards

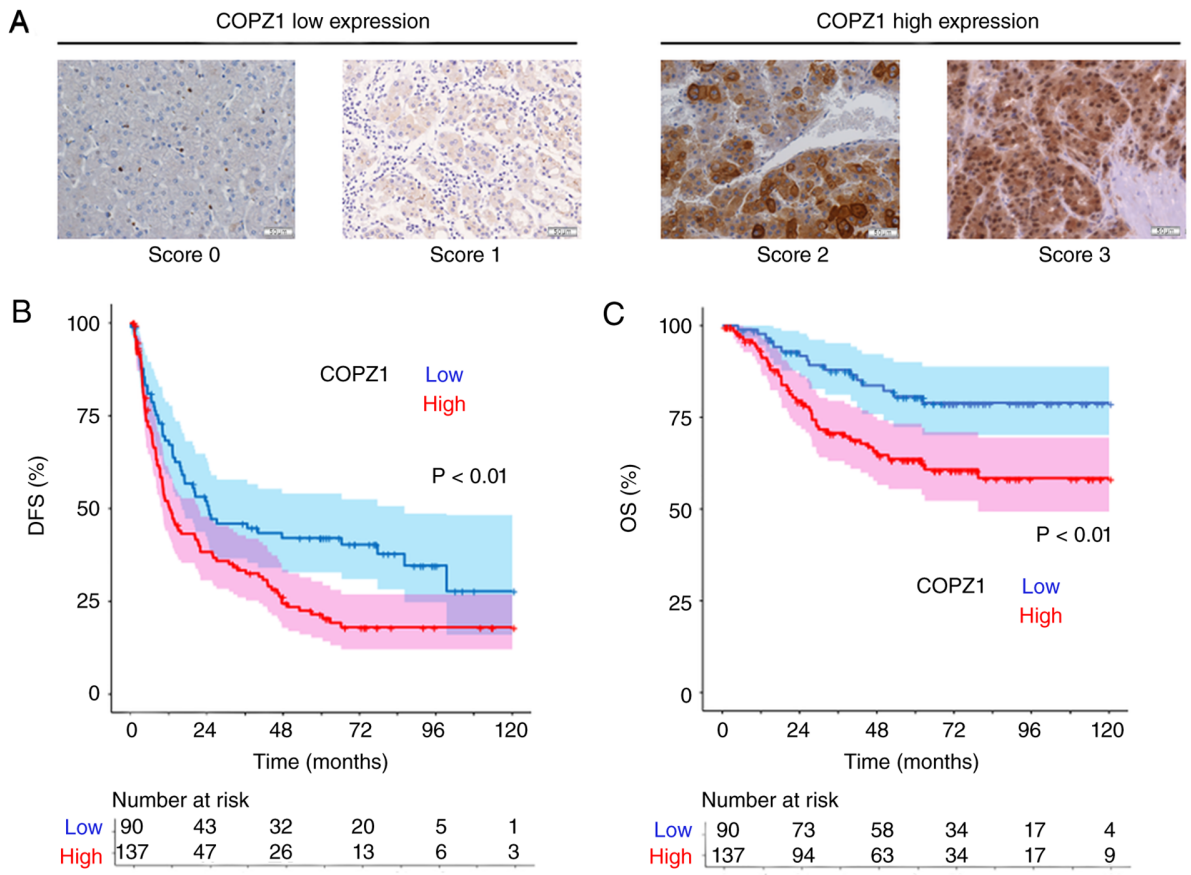


Figure 1. Tumor COPZ1 expression levels are associated with shortened DFS and OS in patients with HCC. (A) Representative immunohistochemistry images showing COPZ1 protein expression in HCC tumor tissues (original magnification: x200). Scale bars, 50 μm. (B) DFS survival curves in 227 patients with HCC who underwent liver resection, stratified into the COPZ1-high (n=137) and COPZ1-low (n=90) groups. (C) OS survival curves for the same groups. Survival curves were estimated using the Kaplan-Meier method and compared using the log-rank test. Shaded areas represent 95% confidence intervals. COPZ1, coatomer protein complex subunit ζ1; DFS, disease-free survival; HCC, hepatocellular carcinoma; OS, overall survival.

assumption was assessed using Schoenfeld residuals. Variables with statistical significance in the univariate analysis were included in the multivariate model. P<0.05 was considered to indicate a statistically significant difference. All analyses were conducted using JMP Pro version 14.0.0 (SAS Institute Inc., Cary, NC, USA).

Results

COPZ1 expression levels are high in the majority of HCC tumors. A total of 227 patients with HCC met the inclusion criteria for this study (Table I). The median follow-up duration was 52.8 months. To validate the specificity of the antibody used for COPZ1 immunostaining, lung cancer cells (LK-2) were used as a positive control and lymphoblast-like cells (SU-DHL-6) served as a negative control. Following successful validation, COPZ1 IHC staining was performed on tumor lesions in HCC specimens. COPZ1 protein expression patterns were scored as 0, 1, 2, or 3 in 52 (22.9%), 38 (16.7%), 125 (55.1%), and 12 (5.3%) of the patients, respectively. Using these scores, all 227 specimens were stratified into the COPZ1-high (n=137, 60.3%) and COPZ1-low (n=90, 39.7%) groups (Fig. 1A). The only significant difference in clinicopathological characteristics between the groups was a higher prevalence of hepatitis C virus (HCV) infection in the COPZ1-high group than in the COPZ1-low group (P=0.011; Table II).

COPZ1 expression is independently associated with DFS and OS following liver resection in patients with HCC. We conducted univariate and multivariate analyses to identify significant prognostic factors for DFS and OS in this cohort. The univariate analysis for DFS showed that high AFP concentrations (P=0.017), elevated des-γ-carboxy prothrombin concentrations (P=0.008), multiple tumors (P=0.003), tumor size >5 cm (P<0.001), presence of vascular invasion (P<0.001), poorly differentiated tumor components (P=0.015), and high COPZ1 expression levels (P=0.006) were significantly associated with poor DFS. The subsequent multivariate analysis incorporating these variables demonstrated that COPZ1 expression was independently associated with shorter DFS (hazard ratio [HR], 1.60; 95% confidence interval [CI], 1.138-2.253; P=0.006). Other factors independently associated with DFS included the tumor size (HR, 1.44; 95% CI, 1.017-2.053; P=0.039) and vascular invasion (HR, 2.00; 95% CI, 1.389-2.881; P<0.001; Table III). The median DFS time was 12.0 months for patients in the COPZ1-high group and 24.1 months for those in the COPZ1-low group (Fig. 1B).

Similar to DFS, the univariate analysis for OS identified AFP concentrations (P=0.001), tumor size (P=0.004),

Table I. Clinical characteristics of patients with HCC (n=227).

Characteristic	Value
Sex	
Male	184
Female	43
Median age, years (range)	66 (34-86)
Viral infection	
HBV	83
HCV	56
HBV + HCV	2
NBNC	86
Child-Pugh classification	
A	219
B	8
AFP	
≤10 ng/ml	104
>10 ng/ml	123
DCP	
≤40 mAU/ml	68
>40 mAU/ml	159
Tumor size	
≤5 cm	122
>5 cm	105
Tumor number	
Solitary	175
Multiple	52
Differentiation	
Well	33
Moderate	143
Poor	51
Vascular invasion	
Positive	67
Negative	160
pStage	
1	16
2	108
3	71
4A	32
4B	0
Cirrhosis	
Positive	55
Negative	172

Data are presented as the number of patients or median (range). AFP, α-fetoprotein; DCP, des-γ-carboxy prothrombin; HBV, hepatitis B virus; HCC, hepatocellular carcinoma; HCV, hepatitis C virus; NBNC, non-HBV non-HCV.

Table II. Association between COPZ1 expression levels and clinicopathological features of patients with HCC (n=227).

Variable	COPZ1-low (n=90)	COPZ1-high (n=137)	P-value
Age			0.954
≤60 years	20 (22.2)	30 (21.9)	
>60 years	70 (77.8)	107 (78.1)	
Sex			0.501
Male	71 (78.9)	113 (82.5)	
Female	19 (21.1)	24 (17.5)	
HBs Ag			0.138
Negative	51 (56.7)	91 (66.4)	
Positive	39 (43.3)	46 (33.6)	
HCV Ab			0.011[a]
Negative	75 (83.3)	94 (68.6)	
Positive	15 (16.7)	43 (31.4)	
AFP			0.542
≤10 ng/ml	39 (43.3)	65 (47.4)	
> 10 ng/ml	51 (56.7)	72 (52.6)	
DCP			0.369
≤40 mAU/ml	30 (33.3)	38 (27.7)	
>40 mAU/ml	60 (66.7)	99 (72.3)	
Differentiation			0.249
Well	17 (18.9)	16 (11.7)	
Moderate	56 (62.2)	87 (63.5)	
Poor	17 (18.9)	34 (24.8)	
Number of tumors			0.131
Single	74 (82.2)	101 (73.7)	
Multiple	16 (17.8)	36 (26.3)	
Tumor size			0.709
≤5 cm	47 (52.2)	75 (54.7)	
>5 cm	43 (47.8)	62 (45.3)	
Vascular invasion			0.896
Negative	63 (70.0)	97 (70.8)	
Positive	27 (30.0)	40 (29.2)	
Cirrhosis			0.224
Negative	72 (80.0)	100 (73.0)	
Positive	18 (20.0)	37 (27.0)	

Data are presented as the number of patients (%). [a]P<0.05. AFP, α-fetoprotein; COPZ1, coatomer protein complex subunit ζ1; DCP, des-γ-carboxy prothrombin; HBs Ag, hepatitis B surface antigen; HCC, hepatocellular carcinoma; HCV Ab, hepatitis C virus antibody.

vascular invasion (P<0.001), tumor differentiation (P<0.001), and COPZ1 expression levels (P=0.004) as potential prognostic factors. In the subsequent multivariate analysis, AFP concentrations (HR, 2.26; 95% CI, 1.271-4.035; P=0.005), vascular invasion (HR, 3.89; 95% CI, 2.293-6.628; P<0.001), poor differentiation (HR, 1.74; 95% CI, 1.012-2.993; P=0.045), and COPZ1 expression levels (HR, 2.60; 95% CI, 1.417-4.773; P=0.002) were independently associated with OS following liver resection (Table III). The proportional hazards assumption was assessed using Schoenfeld residuals. No evidence of violation was observed for COPZ1 in either the DFS or OS analysis, although the assumption was not fully satisfied for

Table III. Univariate and multivariate analyses of DFS and OS (n=227).

A, DFS

	Univariate analysis			Multivariate analysis		
Variable	HR	95% CI	P-value	HR	95% CI	P-value
Sex, Male	1.25	0.828-1.907	0.281			
Age, >60 years	0.92	0.635-1.343	0.679			
HBs Ag, Positive	1.01	0.733-1.410	0.916			
HCV Ab, Positive	0.85	0.592-1.234	0.404			
AFP, >10 ng/ml	1.47	1.070-2.036	0.017[a]	1.23	0.890-1.719	0.205
DCP, >40 mAU/ml	1.61	1.132-2.296	0.008[a]	1.38	0.952-2.001	0.088
Number of tumors, Multiple	1.71	1.196-2.448	0.003[a]	1.43	0.990-2.069	0.056
Tumor size, >5 cm	1.83	1.337-2.527	<0.001[a]	1.44	1.017-2.053	0.039[a]
Vascular invasion, Positive	2.35	1.680-3.297	<0.001[a]	2.00	1.389-2.881	<0.001[a]
Differentiation, Poor	1.58	1.108-2.225	0.015[a]	1.24	0.860-1.810	0.243
Cirrhosis, Positive	1.01	0.702-1.453	0.955			
COPZ1 expression, High	1.59	1.140-2.218	0.006[a]	1.60	1.138-2.253	0.006[a]

B, OS

	Univariate analysis			Multivariate analysis		
Variable	HR	95% CI	P-value	HR	95% CI	P-value
Sex, Male	1.20	0.610-2.367	0.595			
Age, >60 years	0.59	0.347-1.026	0.062			
HBs Ag, Positive	0.96	0.567-1.633	0.887			
HCV Ab, Positive	0.98	0.556-1.741	0.956			
AFP, >10 ng/ml	2.51	1.436-4.405	0.001[a]	2.26	1.271-4.035	0.005[a]
DCP, >40 mAU/ml	1.56	0.875-2.811	0.130			
Number of tumors, Multiple	1.68	0.981-2.905	0.058			
Tumor size, >5 cm	2.09	1.258-3.495	0.004[a]	1.03	0.590-1.830	0.892
Vascular invasion, Positive	4.05	2.446-6.728	<0.001[a]	3.89	2.293-6.628	<0.001[a]
Differentiation, Poor	2.81	1.689-4.694	<0.001[a]	1.74	1.012-2.993	0.045[a]
Cirrhosis, Positive	1.39	0.810-2.396	0.229			
COPZ1 expression, High	2.27	1.287-4.036	0.004[a]	2.60	1.417-4.773	0.002[a]

The numbers of DFS and OS events were 154 and 61, respectively. [a]P<0.05. AFP, α-fetoprotein; CI, confidence interval; COPZ1, coatomer protein complex subunit ζ1; DCP, des-γ-carboxy prothrombin; DFS, disease-free survival; HBs Ag, hepatitis B surface antigen; HCC, hepatocellular carcinoma; HCV Ab, hepatitis C virus antibody; HR, hazard ratio; OS, overall survival.

some clinicopathological covariates. The 5-year OS rate was 63.7% for patients in the COPZ1-high group and 80.1% for those in the COPZ1-low group (Fig. 1C).

Collectively, these findings indicated that COPZ1 expression was independently associated with DFS and OS in the present cohort.

Knocking down COPZ1 expression suppresses cancer cell proliferation, migration, and invasion in HCC cells. To determine the mechanisms underlying the poor prognosis observed in patients with HCC in the COPZ1-high group, we conducted a series of *in vitro* experiments using two human-derived HCC cell lines. As an initial step, COPZ1 expression was silenced in both cell lines using siRNA-mediated knockdown (siCOPZ1) (Fig. 2A). Subsequent experiments were performed using these COPZ1-KD cells and control siRNA-treated cells. Proliferation assays were conducted to examine the effect of COPZ1 expression on HCC cell viability. In PLC/PRF/5 cells, the viability levels at 72 h (0.32 vs. 0.43, P<0.05) and 96 h (0.22 vs. 0.67, P<0.001) were significantly suppressed in the COPZ1-KD cells compared with the control siRNA-treated cells. Cell viability was also significantly suppressed in COPZ1-KD HLF cells compared with the control cells at 96 h (0.41 vs. 0.85, P<0.001). These results indicated that COPZ1 contributed to the growth of HCC cells (Fig. 2B). We next performed wound healing assays to evaluate the effect of COPZ1 expression on

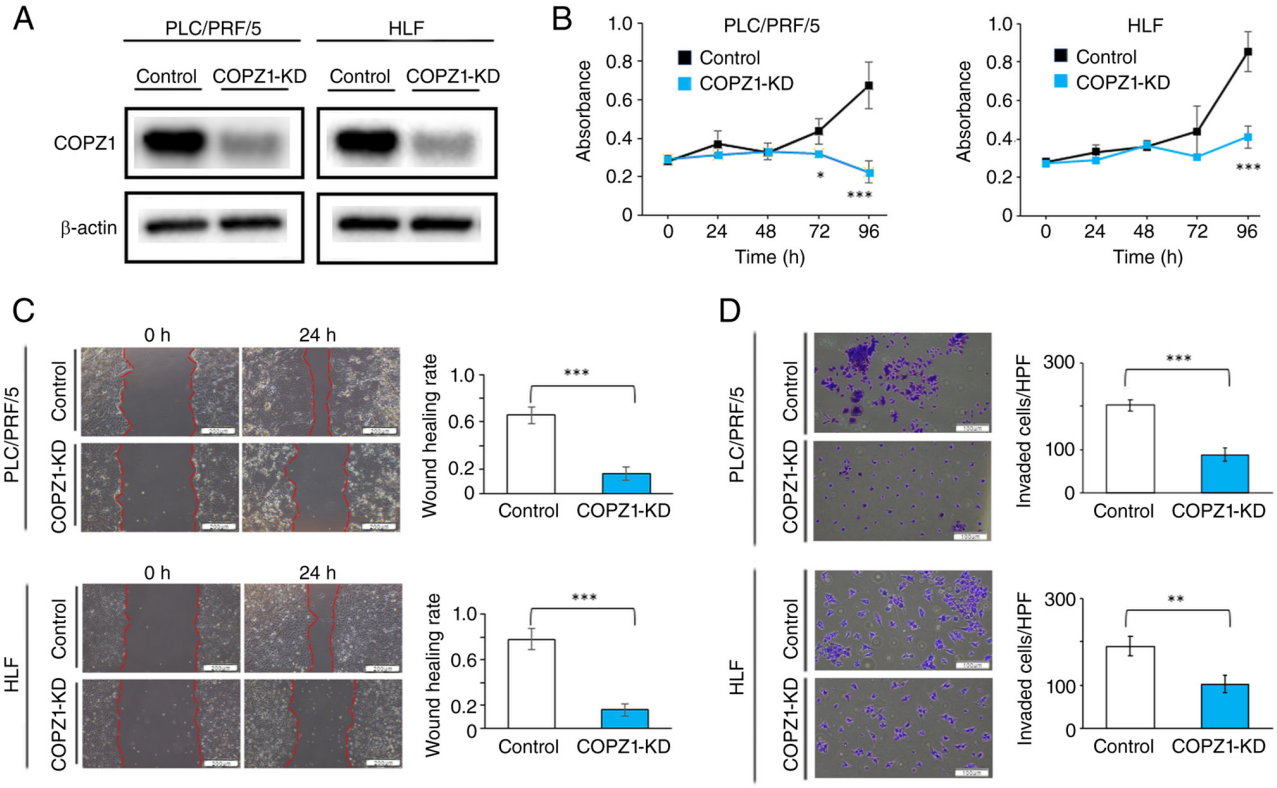


Figure 2. siRNA-mediated KD of COPZ1 suppresses proliferation, migration, and invasion in HCC cells. (A) Western blot analysis shows successful KD of COPZ1 expression in PLC/PRF/5 and HLF HCC cell lines transfected with non-targeting siRNA (control) or COPZ1-targeting siRNA. (B) Proliferation assay comparing PLC/PRF/5 and HLF cell viability between control and COPZ1-KD cells. CCK-8 absorbance was measured at 450 nm. (C) Wound healing assay shows reduced PLC/PRF/5 and HLF cell migration in COPZ1-KD cells compared with control cells. Wound-healing rate was calculated based on the change in wound area from 0 to 24 h. (D) Invasion assay comparing PLC/PRF/5 and HLF cell invasive potential of control and COPZ1-KD cells. Invaded cells were quantified as the number of cells per HPF. All experiments were performed independently three times (n=3 biological replicates). Data are presented as the mean, and error bars indicate the standard deviation. *P<0.05, **P<0.01, ***P<0.001 vs. control, analyzed by Student's t-test. Control, cells transfected with non-targeting control siRNA; COPZ1, coatomer protein complex subunit ζ1; HCC, hepatocellular carcinoma; HPF, high-power field; KD, knockdown; siRNA, small interfering RNA.

HCC cell migration. The migration abilities of PLC/PRF/5 and HLF cells were suppressed in COPZ1-KD cells compared with control siRNA-treated cells (0.16 vs. 0.65, P<0.001; 0.15 vs. 0.78, P<0.001, respectively) (Fig. 2C). Finally, invasion assays showed significantly reduced invasion rates in COPZ1-KD cells compared with control siRNA-treated cells in both cell lines. The invaded cells/high-power field were 88 vs. 202 (P<0.001) in PLC/PRF/5 cells and 103 vs. 190 (P<0.01) in HLF cells (Fig. 2D).

In summary, COPZ1-KD suppressed HCC cell proliferation, migration, and invasion rates.

COPZ1-KD is associated with unfolded protein response-related transcriptional changes in HCC cells. To further evaluate the functional role of COPZ1 in promoting the aggressiveness of HCC cells, we performed a comprehensive genome-wide transcriptomic analysis using RNA-seq in COPZ1-KD and control siRNA-treated cells. To assess the reproducibility of the RNA-seq data, PCA, pairwise Pearson correlation, and BCV analyses were performed (Fig. S2). In PCA using the 500 most variable genes, PC1 separated control from COPZ1-KD samples and accounted for 86.7 and 73.0% of the total variance in HLF and PLC/PRF/5 cells, respectively (Fig. S2A). Pearson correlations between biological replicates were high (r=0.9926-0.9962), and the lowest within-condition correlation exceeded the highest between-condition correlation in both cell lines (Fig. S2B). The median BCV was 11.9% in both cell lines (Fig. S2C). The RNA-seq analysis identified 1,698 and 3,043 DEGs in COPZ1-KD vs. control siRNA-treated HCC cells for PLC/PRF/5 and HLF cells, respectively (Fig. 3A). Among these, 496 DEGs were commonly upregulated in both cell lines.

The enrichment analysis showed significant enrichment of the unfolded protein response (UPR) pathway among the commonly upregulated genes (Fig. 3B and C). This observation was further supported by GSEA of ranked gene expression data from COPZ1-KD vs. control siRNA-treated PLC/PRF/5 cells, which also showed significant enrichment of UPR-related gene sets (Fig. 3D). According to the GSEA rank-metric score, CHAC1, DDIT4, and PSAT1 were the top-ranked UPR-related genes in COPZ1-KD vs. control siRNA-treated cells.

Collectively, these findings suggested that COPZ1-KD was associated with UPR-related transcriptional changes in HCC cells.

COPZ1-KD is associated with ER stress-related changes in HCC cells. On the basis of the finding that the transcriptomic analysis suggested an association between COPZ1-KD and UPR-related changes, we next evaluated key molecules involved in this pathway. Densitometric analysis showed

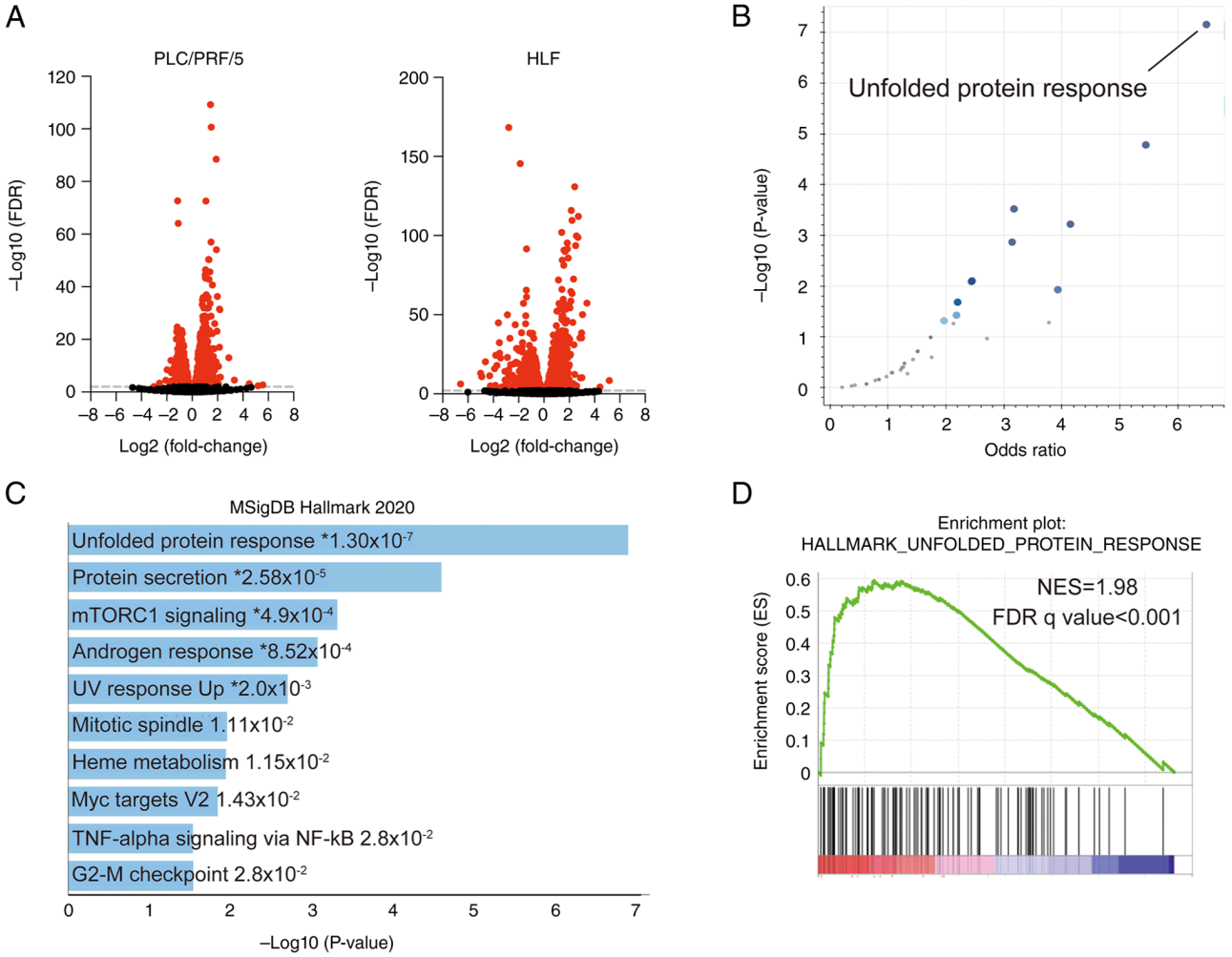


Figure 3. COPZ1-KD is associated with unfolded protein response-related transcriptional changes in HCC cells. (A) Volcano plots showing differentially expressed genes in PLC/PRF/5 and HLF HCC cell lines following COPZ1-KD compared with control cells. (B) Volcano plot of commonly upregulated differentially expressed genes in both cell lines, annotated with the significance of associated gene sets from the Molecular Signatures Database (MSigDB)_ Hallmark_2020 database. (C) Bar chart illustrating the top 10 enriched gene sets from the enrichment analysis using the Enrichr platform. An asterisk (*) indicates adjusted P<0.05. (D) Gene set enrichment analysis shows significant enrichment of unfolded protein response-related gene sets in COPZ1-KD vs. control small interfering RNA-treated PLC/PRF/5 cells. RNA sequencing was performed using two independent biological replicates per condition (n=2). DEGs were identified using a Benjamini-Hochberg adjusted P<0.01. An adjusted P<0.05 was considered statistically significant in the enrichment analysis. Control, cells transfected with non-targeting control siRNA; COPZ1, coatomer protein complex subunit ζ1; DEG, differentially expressed gene; FDR, false discovery rate; HCC, hepatocellular carcinoma; KD, knockdown; NES, normalized enrichment score; siRNA, small interfering RNA.

that GADD34 expression was significantly increased in COPZ1-KD HLF cells compared with control siRNA-treated cells (P=0.0079), whereas PERK, p-PERK, p-eIF2α, and IRE1 showed numerical increases that did not reach statistical significance, and the p-PERK/PERK and p-eIF2α/eIF2α ratios likewise showed no significant difference (Fig. 4A and B). Furthermore, under thapsigargin-induced ER stress, representative fluorescence images qualitatively showed more caspase-3/7-positive cells in COPZ1-KD HLF cells than in control cells (Fig. 4C).

These results suggested that COPZ1-KD was associated with ER stress-related changes in HCC cells.

Discussion

In this study, the IHC analysis of clinical HCC specimens showed that high COPZ1 protein expression levels in tumors were significantly associated with an increased risk of recurrence following liver resection. Functional assays further showed that COPZ1-KD suppressed malignant phenotypes in HCC cell lines. Additionally, COPZ1-KD was associated with UPR-related transcriptional changes and ER stress-related changes in HCC cells. Taken together, these findings indicate that COPZ1 is biologically relevant in HCC, and further investigation of its therapeutic relevance is warranted.

In this study, COPZ1 IHC staining was performed using clinical HCC samples. Wu *et al* (18) reported that high COPZ1 expression was associated with a poor prognosis in patients with lung adenocarcinoma by performing COPZ1 IHC assays using clinical samples. To the best of our knowledge, few previous studies have evaluated COPZ1 expression in clinical HCC samples. In the present cohort, along with other established clinicopathological factors, such as AFP concentrations, tumor size, vascular invasion, and poor differentiation, COPZ1 expression was independently associated with recurrence and OS following liver resection. HCV antibody positivity was more frequent in

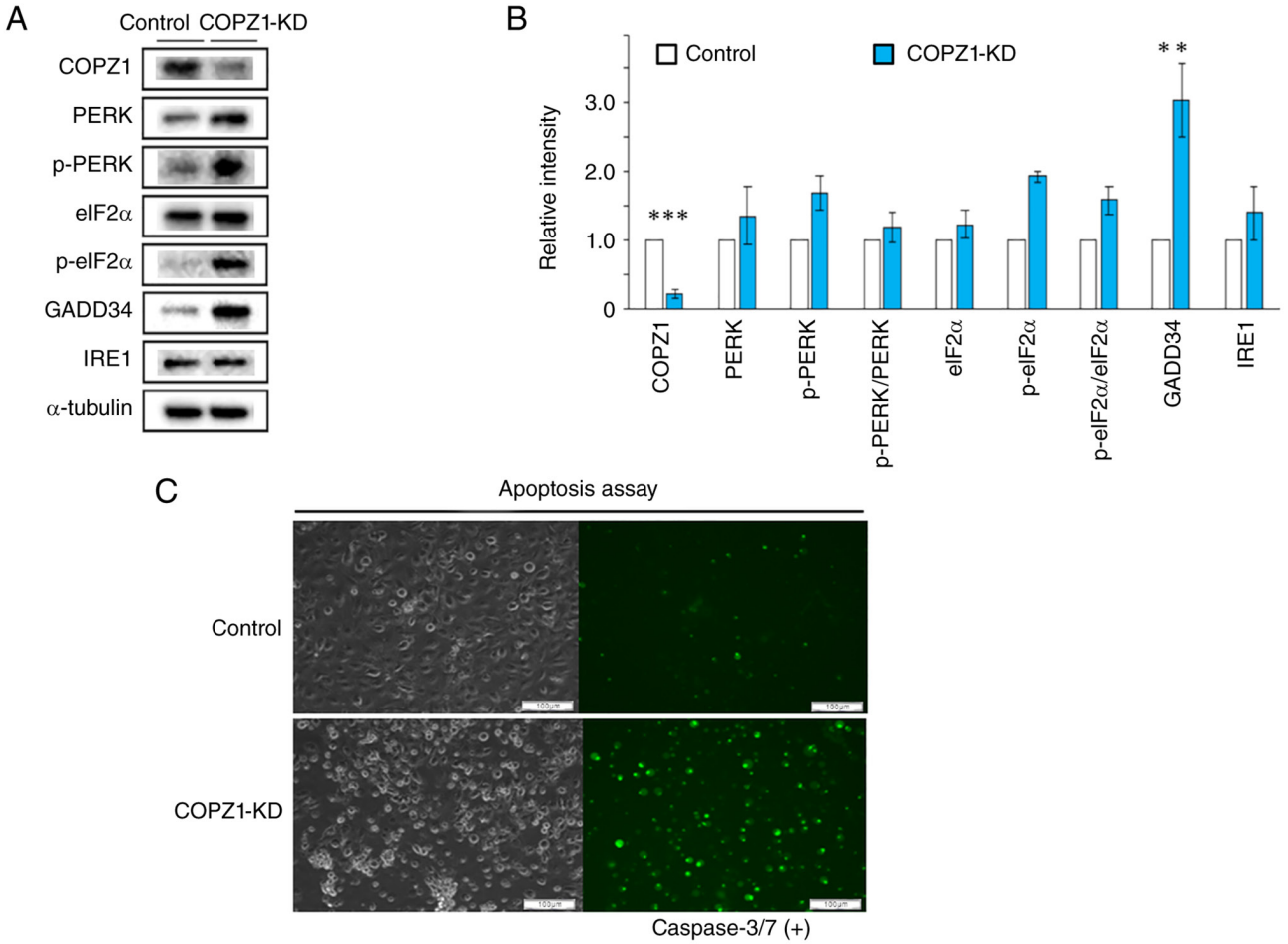


Figure 4. COPZ1-KD is associated with endoplasmic reticulum stress-related changes in hepatocellular carcinoma cells. Under ER stress conditions induced by thapsigargin treatment, the effects of COPZ1-KD were examined. (A) Western blot analysis of ER stress-related proteins in HLF hepatocellular carcinoma cells, with comparison of expression levels between the control and COPZ1-KD groups. (B) Densitometric semi-quantification of the western blot analysis shown in (A). Protein expression levels were normalized to α-tubulin, and p-PERK and p-eIF2α are additionally presented as the ratio to the corresponding total protein (p-PERK/PERK and p-eIF2α/eIF2α). Data are presented as the mean, and error bars indicate the standard deviation. Statistical comparisons between control siRNA-treated and COPZ1-KD cells were performed using Welch's t-test. **P<0.01; ***P<0.001 vs. control. (C) Representative fluorescence images showing caspase-3/7-positive cells in control and COPZ1-KD HLF cells under ER stress conditions. All experiments were performed independently three times (n=3 biological replicates). Control, cells transfected with non-targeting control siRNA; COPZ1, coatomer protein complex subunit ζ1; eIF2α, eukaryotic translation initiation factor 2α; ER, endoplasmic reticulum; GADD34, growth arrest and DNA damage-inducible protein 34; IRE1, inositol-requiring enzyme 1; KD, knockdown; p-, phosphorylated; PERK, protein kinase RNA-like endoplasmic reticulum kinase; siRNA, small interfering RNA.

the COPZ1-high group than in the COPZ1-low group. However, the biological significance of this association remains unclear, and further studies are required to determine whether viral etiology influences COPZ1 expression in HCC. Notably, COPZ1 expression was not clearly correlated with several conventional clinicopathological markers of tumor aggressiveness in the present cohort. This finding suggests that COPZ1 reflects a biological vulnerability or stress-adaptation phenotype that is not fully captured by conventional markers, such as AFP, tumor size, vascular invasion, or histological differentiation.

On the basis of these findings, we performed further *in vitro* investigations using HCC cell lines. The anti-cancer effects of COPZ1-KD in HCC cells prompted us to perform additional analyses, including a comprehensive transcriptomic analysis, to further investigate the underlying mechanisms. These analyses showed that COPZ1-KD was associated with altered expression of genes involved in the UPR and with ER stress-related changes in HCC cells. One possible explanation for this finding is that COPZ1 inhibition impaired COPI complex function, thereby disrupting Golgi-to-ER retrograde transport and promoting unfolded protein accumulation (25). This, in turn, may have triggered ER stress and activated classical UPR pathways (26). When ER stress persists beyond a critical threshold, apoptosis may be triggered as a protective response to limit cellular damage. Although apoptosis may contribute to the decrease in cell viability, the reduced migratory and invasive capacities may reflect UPR-related regulation of cytoskeletal and epithelial-mesenchymal transition signaling. The possibility of this regulation suggests that UPR-related changes induced by COPZ1-KD contribute to reduced tumor cell motility and invasiveness (27). However, the pathway evidence in the present study was primarily based on changes observed following COPZ1-KD and does not establish a direct mechanistic link between COPZ1 and UPR activation.

Although COPZ1 is not an oncogene, it is essential for the survival of a wide variety of cancer cells (28). This phenomenon is known as non-oncogene addiction (29). Our findings

suggest that a subset of HCC depends on COPZ1. Several studies in tumor types other than HCC have suggested that COPZ1 dependency arises in the context of reduced COPZ2 expression (17,28), thereby creating a form of non-oncogene addiction. In these models, suppression of COPZ1 compromises cellular viability, whereas normal cells may tolerate COPZ1 inhibition through compensation by COPZ2 (30,31). However, this proposed mechanism was not directly evaluated in the present study. Additional studies directly examining the COPZ1/COPZ2 relationship will be necessary to clarify whether the vulnerability observed after COPZ1-KD reflects a COPZ2-dependent mechanism in HCC.

In the invasion assay, some invaded cells on the lower surface of the membrane exhibited a rounded appearance. Because transmigration through membrane pores has been shown to involve substantial deformation of the cell body and nucleus (32,33), this appearance may partly reflect such deformation. In the apoptosis assay, green fluorescence was localized to the nuclei of caspase-3/7-positive cells, which additionally showed shrinkage and rounding, morphological features characteristic of apoptosis (34).

This study also has other limitations. First, the clinical cohort was relatively small, and the retrospective single-center design may have introduced selection bias. Therefore, larger multicenter studies are required to further validate the clinical significance of COPZ1 in HCC. Second, the mechanistic findings were derived from *in vitro* experiments alone, and *in vivo* validation is required in future studies. Third, because COPZ1 knockdown reduced cell proliferation, decreased proliferation may have partly contributed to the reduced wound closure observed in the wound-healing assay. Fourth, the RNA-seq analysis was performed using only two biological replicates per condition, which may limit the robustness of the transcriptomic findings, despite the high reproducibility observed between replicates. Fifth, the functional experiments were performed using a single COPZ1-targeting siRNA, and the absence of validation using an additional siRNA or a rescue experiment limits the ability to exclude potential siRNA-specific effects.

In conclusion, this study indicates that COPZ1 is frequently highly expressed in HCC and is independently associated with DFS and OS following liver resection. Functional analyses showed that COPZ1-KD suppressed HCC cell proliferation, migration, and invasion, and was accompanied by ER stress-related changes. These findings support COPZ1 as a biologically relevant candidate vulnerability in HCC, although its therapeutic relevance requires further validation.

Acknowledgements

Not applicable.

Funding

This work was supported by JSPS KAKENHI (grant no. 22K08885).

Availability of data and materials

The RNA-seq data generated in the present study may be found in the DDBJ Sequence Read Archive under accession number DRA028781 and BioProject accession number PRJDB42197 or at the following URL: https://ddbj.nig.ac.jp/search/entry/bioproject/PRJDB42197. Other data supporting the findings of this study are available from the corresponding author upon reasonable request.

Authors' contributions

TKat performed the experiments, collected the data and contributed to drafting the manuscript. TO, YH and AT contributed to the conception and design of the study. YA drafted the manuscript and interpreted the data. KCH performed the pathological evaluation. YF contributed to data analysis. AN, TA and TKak collected patients' specimens and clinicopathological data and contributed to data analysis. AT contributed to the interpretation of the data, supervised the study as the principal investigator. YA and TKat confirm the authenticity of all the raw data. All authors reviewed the manuscript, contributed to the interpretation of the data, and read and approved the final version of the manuscript.

Ethics approval and consent to participate

The present study was approved by the institutional review board of Hokkaido University Hospital (approval no. 019-0060). Informed consent was obtained using an opt-out approach. All analyses of the investigation of clinical data were performed under the ethical guidelines of Hokkaido University.

Patient consent for publication

Not applicable.

Competing interests

The authors declare that they have no competing interests.

Use of artificial intelligence tools

During the preparation of this work, AI tools [ChatGPT (GPT-5.6 Sol; OpenAI)] were used to improve the readability and language of the manuscript, and subsequently, the authors revised and edited the content produced by the AI tools as necessary, taking full responsibility for the ultimate content of the present manuscript.

References

1. Rumgay H, Arnold M, Ferlay J, Lesi O, Cabasag CJ, Vignat J, Laversanne M, McGlynn KA and Soerjomataram I: Global burden of primary liver cancer in 2020 and predictions to 2040. J Hepatol 77: 1598-1606, 2022.
2. Bray F, Laversanne M, Sung H, Ferlay J, Siegel RL, Soerjomataram I and Jemal A: Global cancer statistics 2022: GLOBOCAN estimates of incidence and mortality worldwide for 36 cancers in 185 countries. CA Cancer J Clin 74: 229-263, 2024.
3. Lee YT, Wang JJ, Luu M, Noureddin M, Kosari K, Agopian VG, Rich NE, Lu SC, Tseng HR, Nissen NN, *et al*: The mortality and overall survival trends of primary liver cancer in the United States. J Natl Cancer Inst 113: 1531-1541, 2021.

4. Reig M, Forner A, Rimola J, Ferrer-Fàbrega J, Burrel M, Garcia-Criado Á, Kelley RK, Galle PR, Mazzaferro V, Salem R, *et al*: BCLC strategy for prognosis prediction and treatment recommendation: the 2022 update. J Hepatol 76: 681-693, 2022.
5. Llovet JM, Pinyol R, Yarchoan M, Singal AG, Marron TU, Schwartz M, Pikarsky E, Kudo M and Finn RS: Adjuvant and neoadjuvant immunotherapies in hepatocellular carcinoma. Nat Rev Clin Oncol 21: 294-311, 2024.
6. Martin RC II, Bruenderman E, Cohn A, Piperdi B, Miksad R, Geschwind JF, Goldenberg A, Sanyal A, Zigmont E, Babajanyan S, *et al*: Sorafenib use for recurrent hepatocellular cancer after resection or transplantation: Observations from a US regional analysis of the GIDEON registry. Am J Surg 213: 688-695, 2017.
7. Asahi Y, Kakisaka T, Orimo T, Shimada S, Nagatsu A, Aiyama T, Fujiyoshi S, Sakamoto Y, Fujii Y, Yoshida Y, *et al*: Prognostic significance of Albumin-Bilirubin score changes in patients treated with systemic therapy for recurrent hepatocellular carcinoma after liver resection. Surg Today 56: 1105-1115, 2026.
8. Llovet JM, Ricci S, Mazzaferro V, Hilgard P, Gane E, Blanc JF, de Oliveira AC, Santoro A, Raoul JL, Forner A, *et al*: Sorafenib in advanced hepatocellular carcinoma. N Engl J Med 359: 378-390, 2008.
9. Cheng AL, Kang YK, Chen Z, Tsao CJ, Qin S, Kim JS, Luo R, Feng J, Ye S, Yang TS, *et al*: Efficacy and safety of sorafenib in patients in the Asia-Pacific region with advanced hepatocellular carcinoma: A phase III randomised, double-blind, placebo-controlled trial. Lancet Oncol 10: 25-34, 2009.
10. Kudo M, Finn RS, Qin S, Han KH, Ikeda K, Piscaglia F, Baron A, Park JW, Han G, Jassem J, *et al*: Lenvatinib versus sorafenib in first-line treatment of patients with unresectable hepatocellular carcinoma. Lancet 391: 1163-1173, 2018.
11. Cheng AL, Qin S, Ikeda M, Galle PR, Ducreux M, Kim TY, Lim HY, Kudo M, Breder V, Merle P, *et al*: Updated efficacy and safety data from IMbrave150: Atezolizumab plus bevacizumab vs sorafenib for unresectable hepatocellular carcinoma. J Hepatol 76: 862-873, 2022.
12. Abou-Alfa GK, Lau G, Kudo M, Chan SL, Kelley RK, Furuse J, Sukeepaisarnjaroen W, Kang YK, Van Dao T, De Toni EN, *et al*: Tremelimumab plus durvalumab in unresectable hepatocellular carcinoma. NEJM Evid 1: EVIDoa2100070, 2022.
13. Razi M, Chan EY and Tooze SA: Early endosomes and endosomal coatomer are required for autophagy. J Cell Biol 185: 305-321, 2009.
14. Beller M, Sztalryd C, Southall N, Bell M, Jäckle H, Auld DS and Oliver B: COPI complex is a regulator of lipid homeostasis. PLoS Biol 6: e292, 2008.
15. Zhang Y, Kong Y, Ma Y, Ni S, Wikerholmen T, Xi K, Zhao F, Zhao Z, Wang J, Huang B, *et al*: Loss of COPZ1 induces NCOA4-mediated autophagy and ferroptosis in glioblastoma cell lines. Oncogene 40: 1425-1439, 2021.
16. Beck R, Ravet M, Wieland FT and Cassel D: The COPI system: Molecular mechanisms and function. FEBS Lett 583: 2701-2709, 2009.
17. Anania MC, Cetti E, Lecis D, Todoerti K, Gulino A, Mauro G, Di Marco T, Cleris L, Pagliardini S, Manenti G, *et al*: Targeting COPZ1 non-oncogene addiction counteracts the viability of thyroid tumor cells. Cancer Lett 410: 201-211, 2017.
18. Wu A, Yang H, Xiao T, Gu W, Li H and Chen P: COPZ1 regulates ferroptosis through NCOA4-mediated ferritinophagy in lung adenocarcinoma. Biochim Biophys Acta Gen Subj 1868: 130706, 2024.
19. Orimo T, Ojima H, Hiraoka N, Saito S, Kosuge T, Kakisaka T, Yokoo H, Nakanishi K, Kamiyama T, Todo S, *et al*: Proteomic profiling reveals the prognostic value of adenomatous polyposis coli-end-binding protein 1 in hepatocellular carcinoma. Hepatology 48: 1851-1863, 2008.
20. Aiyama T, Orimo T, Yokoo H, Ohata T, Hatanaka KC, Hatanaka Y, Fukai M, Kamiyama T and Taketomi A: Adenomatous polyposis coli-binding protein end-binding 1 promotes hepatocellular carcinoma growth and metastasis. PLoS One 15: e0239462, 2020.
21. Hu L, Lau SH, Tzang CH, Wen JM, Wang W, Xie D, Huang M, Wang Y, Wu MC, Huang JF, *et al*: Association of vimentin overexpression and hepatocellular carcinoma metastasis. Oncogene 23: 298-302, 2004.
22. Liao J, Li J, Xu J, Xu Y, Wen W, Zheng L and Li L: High S100A9+ cell density predicts a poor prognosis in hepatocellular carcinoma patients after curative resection. Aging (Albany NY) 13: 16367-16380, 2021.
23. Zeng WJ, Liu GY, Xu J, Zhou XD, Zhang YE and Zhang N: Pathological characteristics, PCNA labeling index and DNA index in prognostic evaluation of patients with moderately differentiated hepatocellular carcinoma. World J Gastroenterol 8: 1040-1044, 2002.
24. Kamiyama T, Nakanishi K, Yokoo H, Kamachi H, Tahara M, Yamashita K, Taniguchi M, Shimamura T, Matsushita M and Todo S: Perioperative management of hepatic resection toward zero mortality and morbidity: Analysis of 793 consecutive cases in a single institution. J Am Coll Surg 211: 443-449, 2010.
25. Luo PM and Boyce M: Directing traffic: Regulation of COPI transport by post-translational modifications. Front Cell Dev Biol 7: 190, 2019.
26. Hetz C and Papa FR: The unfolded protein response and cell fate control. Mol Cell 69: 169-181, 2018.
27. Feng YX, Sokol ES, Del Vecchio CA, Sanduja S, Claessen JHL, Proia TA, Jin DX, Reinhardt F, Ploegh HL, Wang Q and Gupta PB: Epithelial-to-mesenchymal transition activates PERK-eIF2α and sensitizes cells to endoplasmic reticulum stress. Cancer Discov 4: 702-715, 2014.
28. Shtutman M, Baig M, Levina E, Hurteau G, Lim CU, Broude E, Nikiforov M, Harkins TT, Carmack CS, Ding Y, *et al*: Tumor-specific silencing of COPZ2 gene encoding coatomer protein complex subunit ζ2 renders tumor cells dependent on its paralogous gene COPZ1. Proc Natl Acad Sci USA 108: 12449-12454, 2011.
29. Di Marco T, Bianchi F, Sfondrini L, Todoerti K, Bongarzone I, Maffioli EM, Tedeschi G, Mazzoni M, Pagliardini S, Pellegrini S, *et al*: COPZ1 depletion in thyroid tumor cells triggers type I IFN response and immunogenic cell death. Cancer Lett 476: 106-119, 2020.
30. Shtutman M and Roninson IB: A subunit of coatomer protein complex offers a novel tumor-specific target through a surprising mechanism. Autophagy 7: 1551-1552, 2011.
31. Di Marco T, Vergaro D and Greco A: COPZ1: An example of non-oncogene addiction in human tumors. Front Pharmacol 16: 1636326, 2025.
32. Kramer N, Walzl A, Unger C, Rosner M, Krupitza G, Hengstschläger M and Dolznig H: In vitro cell migration and invasion assays. Mutat Res 752: 10-24, 2013.
33. Wolf K, te Lindert M, Krause M, Alexander S, te Riet J, Willis AL, Hoffman RM, Figdor CG, Weiss SJ and Friedl P: Physical limits of cell migration: Control by ECM space and nuclear deformation and tuning by proteolysis and traction force. J Cell Biol 201: 1069-1084, 2013.
34. Elmore S: Apoptosis: A review of programmed cell death. Toxicol Pathol 35: 495-516, 2007.

Copyright © 2026 Kato et al. This work is licensed under a Creative Commons Attribution-NonCommercial-NoDerivatives 4.0 International (CC BY-NC-ND 4.0) License.